Journal of Cardiovascular Magnetic Resonance (2007) **9,** 63–70

ISSN: 1097-6647 print / 1532-429X online
DOI: 10.1080/10976640600843462

informa
healthcare

Comparison of Gadolinium-Enhanced Cardiovascular Magnetic Resonance Angiography with High-Resolution Black Blood Cardiovascular Magnetic Resonance for Assessing Carotid Artery Stenosis

Lukasz S. Babiarz, BA,[1] Brad Astor, PhD, MPH,[2] Mona A. Mohamed, MD, PhD,[1] and Bruce A. Wasserman, MD[1]

The Russell H. Morgan Department of Radiology, and Radiological Sciences, The Johns Hopkins Hospital, Baltimore, Maryland, USA[1]
The Johns Hopkins Bloomberg School of Public Health, Baltimore, Maryland, USA[2]

ABSTRACT

***Purpose*: Carotid angiography is used to assess stroke risk, but it cannot reliably characterize plaque burden because the vessel remodels during plaque formation. High-resolution black blood cardiovascular magnetic resonance (BBCMR) depicts the outer wall thereby providing a truer estimate of plaque size. We compared carotid stenosis by gadolinium enhancement cardiovascular magnetic resonance angiography (CMRA) versus high-resolution BBCMR. *Methods*: Twenty-four subjects (M:F = 20:4; ages 57–83 years) with carotid atherosclerosis underwent CMRA and transaxial BBCMR through the stenosis. Area and diameter stenosis measurements by NASCET criteria using CMRA images were compared to area stenosis measurements based on outer wall and lumen contours drawn on corresponding BBCMR images. *Results*: Area stenosis by CMRA correlated with area stenosis by BBCMR (r = 0.77; 95% CI: 0.58, 0.89). BBCMR values exceeded corresponding CMRA area measurements in 20 of 24 cases, with the remainder being highly stenotic (>90%). *Conclusion*: CMRA yields lower estimates of luminal narrowing compared to BBCMR, which delineates the outer wall and accounts for vascular remodeling. BBCMR could serve as a new measure of narrowing to guide management, but prospective studies are needed to better understand the clinical implications of this new scale of disease.**

Received 20 February 2006; accepted 25 May 2006.
Keywords: Atherosclerosis, Carotid Stenosis, Carotid Artery Plaque, Magnetic Resonance Angiography, Cardiovascular Magnetic Resonance, Remodeling.
This study was supported in part by the Johns Hopkins University School of Medicine General Clinical Research Center grant number M01-RR00052, from the National Center for Research Resources/National Institutes of Health. The authors would like to thank Dr. Thomas Foo and Dr. Glenn Slavin for their technical support in this study.
Correspondence to:
Bruce A. Wasserman, MD
The Russell H. Morgan Department of Radiology and Radiological Sciences
The Johns Hopkins Hospital
600 N. Wolfe Street
Phipps B-100,
Baltimore, MD 21287
tel: 410-614-9200; fax: 410-614-1213
email: bwasser@jhmi.edu

INTRODUCTION

Atherosclerotic disease in the proximal internal carotid artery (ICA) and carotid bulb is frequently associated with thromboembolic events that cause stroke. The North American Symptomatic Carotid Endarterectomy Trial (NASCET) demonstrated a significant reduction in stroke risk with carotid endarterectomy compared to medical management for patients with symptomatic high-grade stenosis (i.e., 70 to 99%) (1, 2). The European Carotid Surgery Trial (ECST) similarly showed a beneficial outcome for surgical intervention in symptomatic patients with carotid narrowing greater than 69% (3). These studies helped to establish endarterectomy as the standard of care for treating symptomatic carotid disease with narrowing greater than or equal to 70% (4).

Both NASCET and ECST utilized catheter-based conventional angiography to determine the degree of narrowing caused by atheroma. Both methods measured stenosis at the point of greatest narrowing; however, NASCET used the distal ICA

beyond any poststenotic dilatation as the reference diameter, whereas the extrapolated lumen at the point of greatest narrowing was used in ECST. This extrapolated reference diameter was the basis for the poor interobserver agreement for stenosis measurements using the ESCT approach (5). On the other hand, the NASCET measurement can result in zero or negative stenosis since the reference diameter can be smaller than the diameter at the point of greatest narrowing, as is often the case in the carotid bulb lesions (6). For bulb lesions, application of the common carotid artery (CCA) method (7) in which the CCA lumen is taken as the reference diameter might give a more accurate assessment of narrowing.

Gadolinium enhanced cardiovascular magnetic resonance angiography (CMRA) is increasingly preferred over digital subtraction angiography (DSA) for assessing carotid stenosis because of its lower risk and comparable accuracy (8, 9). When CMRA is used to assess carotid disease, the NASCET method is often applied since it offers the highest sensitivity for detecting severe stenosis (10).

Although angiography, specifically DSA, MRA, or computed tomography angiography (CTA), has become the standard approach to carotid artery disease assessment, it is limited by its inability to depict the outer wall of the vessel. As atherosclerosis develops, the artery dilates in response to changes in shear stress experienced by the endothelial cells. This vascular remodeling leads to normalization of the luminal diameter, which normalizes the shear stress (11–13). In coronary arteries, Glagov et al. documented that atheroma can occupy up to 40% of the internal elastic lamina (IEL) area before any stenosis is detected by angiography (14). Therefore, early plaque formation is angiographically occult. More advanced disease is thus underestimated by angiography since this measures plaque burden by its effect on the lumen. Compensatory dilatation has also been demonstrated in carotid arteries (15–17). Benes et al. (16) showed that angiography underestimates carotid artery narrowing based on a comparison with corresponding endarterectomy specimens. However, endarterectomy studies cannot assess the degree of underestimation due to the incompleteness of the resected plaque and its shrinkage following removal (18). The degree of this underestimation by angiography has not been studied *in vivo* in human arteries.

High-resolution black blood cardiovascular magnetic resonance (BBCMR) can depict the actual plaque size by imaging both the lumen and outer wall of an artery. Studies comparing *in vivo* BBCMR with corresponding endarterectomy specimens confirm the ability of BBCMR to accurately depict atheroma size (19). This technique can provide a more accurate characterization of plaque burden that gives insight into the underestimation limiting angiography (20).

The aims of this study were: 1) to determine the relationship between luminal stenosis by CMRA with stenosis by BBCMR, which accounts for vascular remodeling; 2) to determine the degree of narrowing measured by BBCMR that is equivalent to 70% by NASCET in order to better understand the clinical implication of measurements by this new technique; and 3) to determine whether stenosis measured by CMRA using the CCA as the reference diameter more closely reflects narrowing measured by BBCMR for bulb lesions.

MATERIALS AND METHODS

Study population

Thirty-seven consecutive subjects underwent CMR evaluation for carotid artery stenosis which included CMRA and BBCMR of only the stenotic side between April 25, 2000 and December 16, 2002. Subjects were referred based on a recent ultrasound or CMRA evaluation showing carotid narrowing. Twenty-four subjects were included in this study (20 men and 4 women; mean age, 70.5 $\pm$ 8.1 years, range 57–83; 11 right carotid arteries, 13 left carotid arteries). The remaining 13 were excluded because no atherosclerotic plaque was visualized in the carotid bifurcation (3 studies), the BBCMR sequence did not cover the point of greatest narrowing (2 studies), data was missing (1 study), and poor image quality (motion artifact on the CMRA study in 1 exam, missed arterial phase with venous contamination on the CMRA sequence in 1 study, and BBCMR slices were acquired obliquely through the plaque resulting in artifactual wall thickening in 5 studies). Informed consent was obtained for this study as part of a protocol approved by the local Institutional Review Board.

CMR

MR imaging was performed using a 1.5-T MR scanner (GE Medical Systems, Milwaukee, Wisconsin, USA) with a dual 3 inch (7.6 cm) surface coil (GE Medical Systems), immobilized by a mechanical support. The carotid bifurcation was localized using fast gradient echo multiplanar sequences and the point of narrowing was identified by either a two-dimensional or three-dimensional time-of-flight (TOF) MR angiogram. Black blood images were acquired using a cardiac-gated, double inversion-recovery, fast spin-echo pulse sequence (21). First, a proton-density- (PD-) weighted oblique BBCMR image was acquired through the carotid bifurcation to include the long axis of the vessel (Fig. 1a), and this was used as a scout image to orient four or five transverse T1- and PD-weighted BBCMR images through the plaque (Fig. 1b–c). The transverse BBCMR images were acquired with fat suppression and were oriented perpendicular to the long axis of the vessel as described by Wasserman et al. (22) The slices were centered at the level of greatest stenosis. This double oblique approach was used to minimize the partial volume averaging effects on the lumen and outer wall measurements, as well as to maximize the time-of-flight flow void effect on the lumen.

Imaging parameters were as follows: slice thickness, 2 mm; 0 gap; matrix, 256 $\times$ 256; field of view, 14 cm; echo train length, 32; and one signal acquired. All images were gated by electrocardiography or pulse, with a TR equal to the duration of two cardiac cycles for the PD-weighted images and one cycle for the T1-weighted images (approximate imaging time: 30 and 15 seconds per slice, respectively). The echo time was set to 5 ms for all black

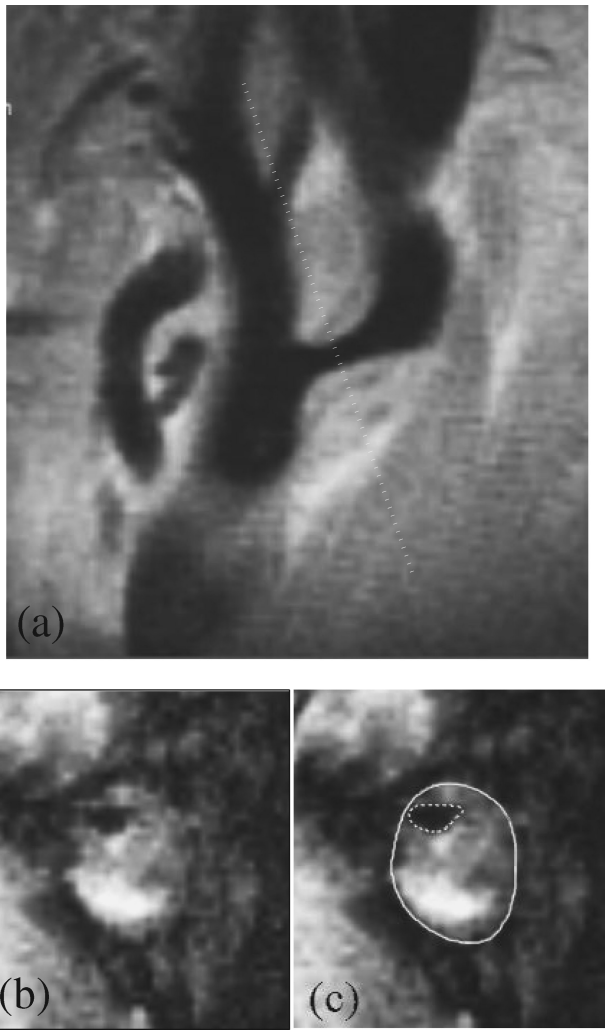

Figure 1. BBCMR images through plaque in the carotid bulb. **a**) Oblique BBCMR image through the long axis of the carotid bifurcation with a line indicating the orientation of the transverse image to follow, **b**) transverse postcontrast T1-weighted BBCMR image through the plaque at the point of greatest narrowing, **c**) outer wall (solid circle) and lumen (broken circle) contours are drawn using semiautomated software (VesselMASS, Leiden University).

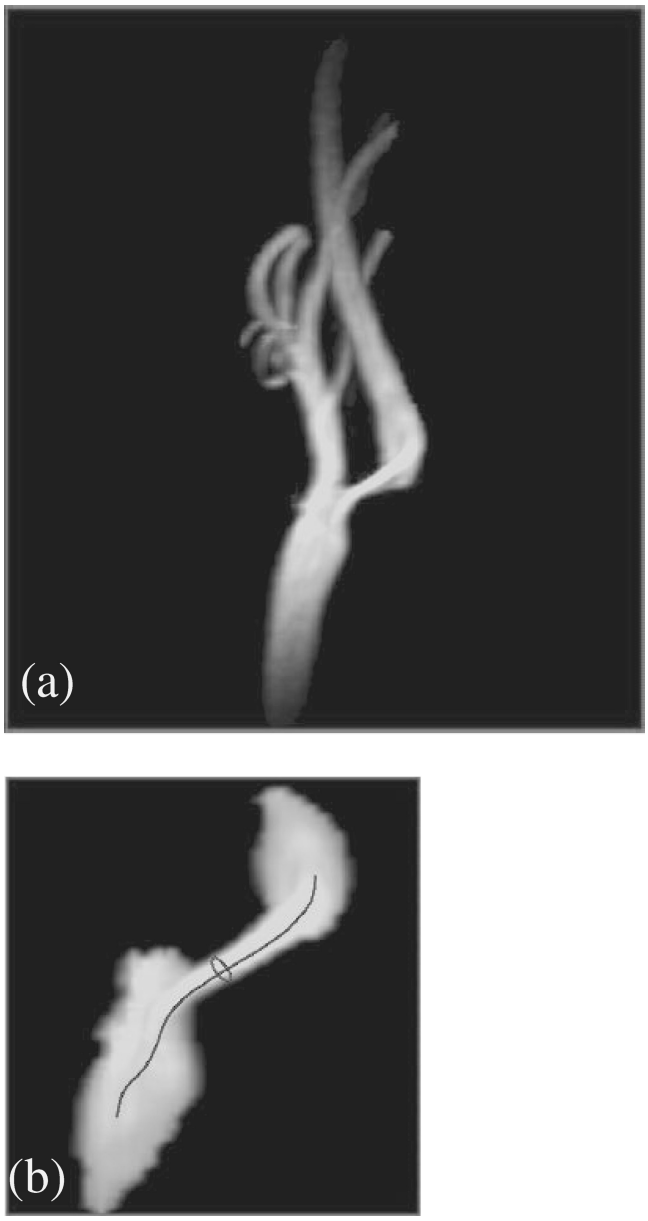

Figure 2. CMRA images that correspond with the vessel in Figure 1. **a**) Maximum intensity projection (MIP) of the carotid bifurcation, **b**) The center-point of the stenotic segment is delineated (line) and the lumen is outlined at the point of greatest narrowing (circle) using semiautomated software (Volume Analysis, GE Medical Systems).

blood images. The inversion time was set to approximately 600 ms for PD-weighted images (TR = 2RR intervals) and approximately 360 ms for T1-weighted images (TR = 1RR interval) to minimize the blood pool signal on the basis of estimated T1 values of blood and accounting for variations in heart rate.

Gadopentetate dimeglumine (Magnevist; Berlex Laboratories, Wayne, New Jersey, USA), 0.1 mmol per kilogram of body weight, was injected intravenously using a power injector at 2 mL/s, and the T1-weighted transverse acquisition was repeated approximately 5 minutes after the injection. The inversion time was adjusted to 200 ms to account for gadolinium administration. A 3D CMR angiogram was acquired as a mask and then again during the arterial phase of the contrast injection (Fig. 2a). This scan was acquired in the coronal plane using a spoiled gradient echo (SPGR) sequence with the following parameters: TR/TE, 6.5/1.6; flip angle, 45°; full bandwidth, 62.5 kHz; matrix, 256 × 128; field of view, 16 × 12.8 cm; slice thickness, 2 mm; partitions, 46; and acquired voxel size, 0.625 × 1.25 × 2 mm. K-space was ordered using a 3D elliptical centric view order. The images were reconstructed by zero filling to a matrix size of 256 × 256, and the 46 partitions acquired at 2 mm were interpolated to 92 partitions. Acquisition time was approximately 30 s per 3D slab, and a total of 3 acquisitions (phases) were

acquired. Because surface coils were used, the aortic arch was not visualized. The first of 3 phases was acquired 10 seconds after contrast administration which enabled excellent luminal enhancement of the carotid artery for all cases.

Image analysis

CMRA images were evaluated for degree of stenosis based on minimum diameter and minimum area using the NASCET method to determine the location of the reference measurement (i.e., using the ICA beyond the narrowing and any poststenotic dilatation for reference) (23). The bottom limit of the carotid bulb was defined as where the common carotid artery begins to dilate and the vessel walls curve out. The upper limit, which marks the origin of the internal carotid artery, was defined at or beyond the tip of the flow divider where the outward curve of the carotid wall straightens. All diameter and area measurements were oriented orthogonal to the vessel axis and were acquired using semiautomated software (Volume Analysis, Voxtool 3.0.404; GE Medical Systems) (Figs. 2 a and b). The point of maximum stenosis was determined by the software, whereas the level of the reference diameter was user-defined. The automated software provided lumen area and diameter measurements at both levels of interest. When diameter- or area-based stenosis resulted in a negative value, stenosis was recorded as 0%. Diameter stenosis was calculated according to the formula [1 – sD/rD]* 100%, where sD is the minimum diameter measurement at the point of greatest narrowing and rD is the diameter at the reference location. Area stenosis was determined by the formula [1–sA/rA]* 100% where sA represents the lumen area at the most stenotic point and rA represents the lumen area at the reference location. For subjects with carotid bulb lesions (n = 3), stenosis was also evaluated using the CCA diameter or area just below the carotid bifurcation as the reference location in place of the distal ICA measurements beyond the narrowing (7). The distance between the point of greatest narrowing and the reference point was recorded.

Outer wall and lumen contours were drawn on the BBCMR images at the point of greatest narrowing by a radiologist blinded to the objectives of this study and trained to perform this analysis using Vesselmass software (VesselMASS, Division of Image Processing, Radiology Department, Leiden University Medical Center, the Netherlands) (Fig. 1b–c). The outer wall contour was drawn on the postcontrast T1-weighted BBCMR, which was used based on reports that gadolinium-enhancement improves delineation of the outer wall (22, 24). The PD-weighted image was used to confirm the contour of the outer wall in areas in which gadolinium enhancement was not as apparent. The precontrast T1-weighted image was used to confirm the lumen contour for cases in which lumen delineation was obscured by flow artifact caused by contrast administration. For each study, the area of the lumen and the area enclosed by the outer vessel wall were determined, and wall area and percent stenosis by BBCMR were calculated as follows: Wall area = Outer vessel wall area – Lumen area; Percent stenosis by BBCMR = [Wall Area/Outer vessel wall area] ∗ 100%.

Statistical methods

Area and diameter stenosis measurements using CMRA images were compared to area stenosis measurements based on corresponding BBCMR images. The linearity and agreement of stenosis measurements based on the CMRA and BBCMR methods were evaluated by correlation coefficients and linear regression models, fitting BBCMR results to CMRA results. These analyses were performed using the NASCET method for determining the location of the reference measurement for the entire group (n = 24) and repeated using the CCA as the reference diameter for the 3 bulb lesions and NASCET for the remainder. The BBCMR values (and 95% confidence intervals) at 0% and 70% diameter stenosis by CMRA were predicted from these models. Interobserver variation of BBCMR percent stenosis was assessed by duplicate readings in 10 subjects. Intraobserver variation was assessed by duplicate readings in 6 subjects. The mean percentage difference between readings was calculated.

RESULTS

Compared with stenosis based on area measurements on BBCMR images, stenosis based on CMRA images using the NASCET method for determining the location of the reference measurement was lower in 23 out of 24 cases using diameter measurements and 20 out of 24 cases using area measurements. All the cases that were not lower were highly stenotic (greater than 90% narrowing on both CMRA and BBCMR). Stenosis based on CMRA measurements resulted in a negative value for only one case, and for this case both area- and diameter-based calculations were negative and reported as zero. The mean percentage error between observers for BBCMR percent stensosis was 4.5% (range: 0.7 to 9.2%). The mean percentage error between duplicate measurements by the same reader was 1.0% (range: 0.1 to 1.7%).

A stenosis of 0% by diameter measurements on CMRA corresponded to 67.3% (95% CI: 60.1, 74.4) by BBCMR (Fig. 3). This estimate was 62.6% (95% CI: 54.5, 70.8) when stenoses for the 3 bulb lesions were measured using the CCA as the reference diameter (Fig. 3). A stenosis of 70% by diameter measurements on CMRA corresponded to 89.4% (95% CI: 85.1, 93.6) by BBCMR. This estimate was 89.7% (95% CI: 85.7, 93.7) when stenoses for the 3 bulb lesions were measured using the CCA as the reference diameter.

A stenosis of 0% by area measurements on CMRA corresponded to 63.1% (95% CI: 54.6, 71.6) by BBCMR (Fig. 4). This estimate was 51.5% (95% CI: 42.7, 60.3) when stenoses for the 3 bulb lesions were measured using the CCA as the reference area (Fig. 4). Percent stenosis based on CMRA area measurements using the NASCET method for determining the location of the reference measurement correlated with stenosis determined by BBCMR (r = 0.77; 95% CI: 0.58, 0.89). When stenoses for the 3 bulb lesions were measured using the CCA as the reference area, stenoses determined by CMRA correlated better with BBCMR narrowing measurements (r = 0.87; 95% CI: 0.73, 0.94); however, the difference in the value

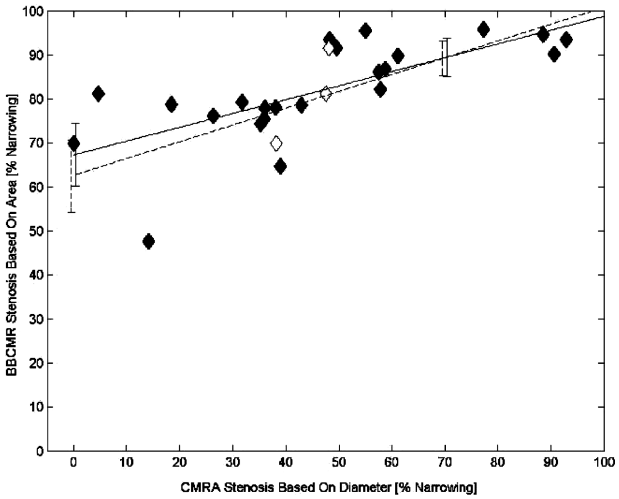

Figure 3. Linear regression for BBCMR area-based stenosis measurements as a function of CMRA diameter-based stenosis measurements. CMRA stenosis was measured using the distal ICA beyond the narrowing as the reference diameter (NASCET method; solid line) and repeated using the CCA as the reference diameter for the 3 bulb lesions and the NASCET method for the remainder (dashed line). Closed black diamond = ICA lesion stenosis measured using NASCET method; closed gray diamond = CCA lesion stenosis measured using NASCET method; open diamond = CCA lesion stenosis measured using CCA as the reference diameter. A stenosis of 0% by CMRA corresponded to 67.3% (95% CI: 60.1, 74.4) by BBCMR (solid line). This estimate was 62.6% (95% CI: 54.5, 70.8) when stenoses for the 3 bulb lesions were measured using the CCA as the reference diameter (dashed line). A stenosis of 70% on CMRA corresponded to 89.4% (95% CI: 85.1, 93.6) by BBCMR (solid line). This estimate was 89.7% (95% CI: 85.7, 93.7) when stenoses for the 3 bulb lesions were measured using the CCA as the reference diameter (dashed line). The Pearson correlation coefficient for this regression was 0.75 (solid line), and when the 3 bulb lesion stenoses were evaluated using the CCA as the reference diameter it was 0.77 (dashed line).

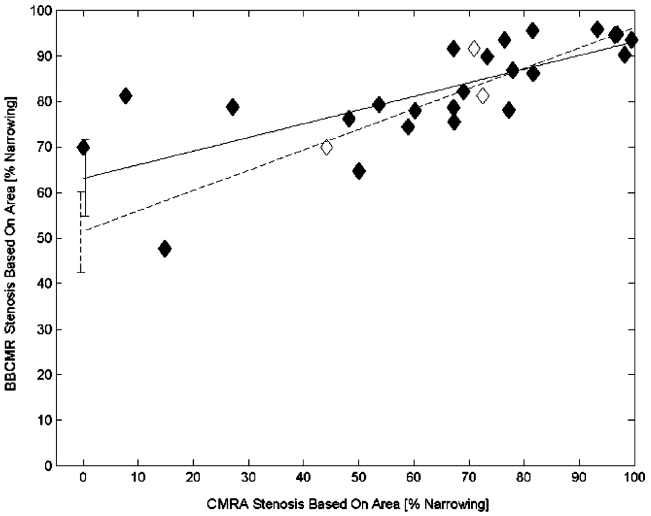

Figure 4. Linear regression for BBCMR area-based stenosis measurements as a function of CMRA area-based stenosis measurements. CMRA stenosis was measured using the distal ICA beyond the narrowing as the reference area (NASCET method; solid line) and repeated using the CCA as the reference area for the 3 bulb lesions and the NASCET method for the remainder (dashed line). Closed black diamond = ICA lesion stenosis measured using NASCET method; closed gray diamond = CCA lesion stenosis measured using NASCET method; open diamond = CCA lesion stenosis measured using CCA as the reference diameter. A stenosis of 0% by CMRA corresponded to 63.1% (95% CI: 54.6, 71.6) by BBCMR (solid line). This estimate was 51.5% (95% CI: 42.7, 60.3) when stenoses for the 3 bulb lesions were measured using the CCA as the reference diameter (dashed line). The Pearson correlation coefficient for this regression was 0.74 (solid line), and when the 3 bulb lesion stenoses were evaluated using the CCA as the reference diameter it was 0.83 (dashed line).

of the Pearson correlation coefficient was not significant ($p = 0.14$).

The degree of underestimation, that is the difference between stenoses by area measurements based on CMRA and on BBCMR, was not associated with the distance between the point of narrowing and the reference diameter used for the ICA lesions. The mean distance between the point of greatest narrowing and the reference diameter for the 21 plaques in the proximal ICA beyond the bulb was 7.5 mm (SD = 4.0; min = 2.1, max = 17.0). For the 3 bulb lesions, this mean distance was 19.6 mm (16.4, 19.2, 23.2) when the NASCET method was used, and 8.4 mm (3.8, 5.9, 15.5) when the CCA was used as the reference diameter. Distance from the most stenotic point to the reference point is regressed against the difference between stenosis by BBCMR and stenosis by CMRA in Figure 5. The 3 bulb lesion stenoses are outliers when evaluated using the NASCET method for determining the location of the reference measurement, and they fit the pattern of the other data points when evaluated using the CCA as the reference diameter.

DISCUSSION

We have shown that measurements of carotid stenosis by BBCMR reveal a lower estimate of stenosis on corresponding CMRA images with narrowing of 67.3% (95% CI: 60.1, 74.4) on the BBCMR image corresponding to no stenosis on the CMRA study using the NASCET method. This difference was expected because BBCMR can delineate the outer wall and account for the outward remodeling of the vessel that occurs during atheroma development that is not detectable by angiography. This outward remodeling preserves the lumen size so that early disease cannot be identified by modalities that rely on luminal narrowing for detection. The normal tapering of the vessel between the point of narrowing and the reference diameter may contribute to this underestimation; however, in our study, there was no association between the degree of underestimation and the distance between the point of narrowing and the reference diameter used for the ICA lesions. In other words, we did not observe the greater underestimation that might be expected with NASCET measurements of CMRA due to the normal tapering of the vessel for longer lesions (i.e., longer distance between narrowing and reference diameter). Interpretation of percent stenosis measured by BBCMR in vessels without plaque formation must consider the

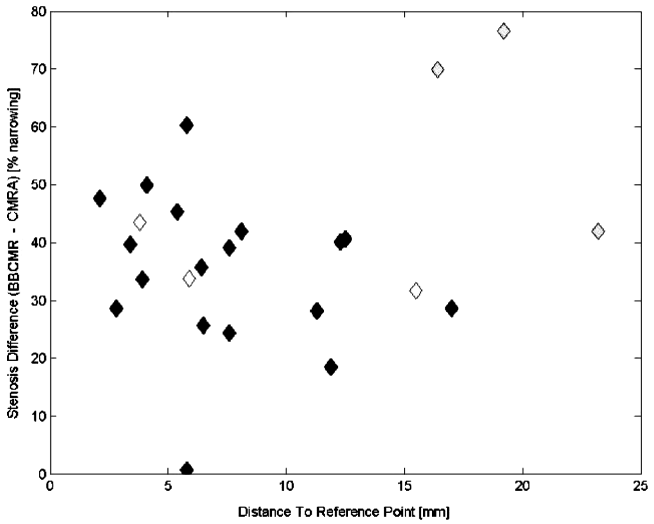

Figure 5. Scatter plot for stenosis difference between BBCMR and CMRA as a function of distance to the reference point. Closed black diamond = ICA lesion stenosis measured using NASCET criteria; closed gray diamond = CCA lesion stenosis measured using NASCET criteria; open diamond = CCA lesion stenosis measured using CCA as the reference diameter. When the 3 bulb lesion stenoses were evaluated according to NASCET method they were data outliers. When the same 3 bulb lesion stenoses were evaluated using the CCA as the reference diameter they fit the pattern of the other data points.

inclusion of the vessel wall in the calculation. The vessel wall can account for between 20 to 30% of the area circumscribed by its outer wall.

We used CMRA rather than conventional DSA for measurements of luminal narrowing. CMRA has become a widely-accepted noninvasive alternative to DSA with comparable accuracy and sensitivity (8, 9). We know that CMRA images may overestimate stenosis due to dephasing artifact along the margin of the lumen, which becomes exaggerated in areas of tight narrowing, and because of the signal intensity threshold used to create the Maximum Intensity Projections (MIP). CMRA has been shown to overestimate the severity of stenosis compared to conventional 3D TOF CMRA (25), and CMRA has been shown to overestimate luminal narrowing compared to conventional angiography and DSA (26). This further supports our conclusion that stenosis is underestimated on CMRA since it is observed despite these inherent reasons for overestimation. Furthermore, the overestimation that limits CMRA may lead to surgical management for some who are not surgical candidates based on studies originally used to validate NASCET and ECST. BBCMR is not subject to these technical limitations that alter the measured stenosis, and may serve as a more accurate measure of narrowing though it should be noted that incomplete suppression of blood signal near the wall can lead to higher estimates of stenosis, highlighting the need to select the appropriate inversion time. CMRA remains the preferred approach to lumen assessment by CMR at many institutions since, compared to TOF techniques, it is less affected by signal loss from saturation effects and can therefore provide much better coverage, more reliably identify ulcers, and more reliably distinguish occlusion from severe stenosis, so our comparison to this method has greater practical applicability.

Our study suggests that a large plaque burden may be present despite an unalarming angiographic appearance. This may explain the moderate risk for stroke seen in less severe carotid stenosis (2). A new stratification for stenoses will be needed for this method to be applicable to surgical management similar to that used in NASCET or ECST. Until population-based prospective trials are completed and reveal clinically relevant measures of narrowing by BBCMR, CMRA will remain the more relevant measure to predict events and guide management.

Measurements of stenosis by the ECST method are generally higher than that by NASCET, since the ECST method extrapolates the diameter of the outer wall, and this might be considered more similar to our method. However, the extrapolation of the outer wall likely accounts for the poor reader variability reported by Griffiths et al. (5), and this limitation is averted with BBCMR. Rothwell et al. (27) reanalyzed the results of the ECST and found that, on average, 50% and 70% stenosis by the NASCET method were equivalent to 65% and 82% stenosis, respectively, by the ECST method. We determined that 89% narrowing by BBCMR corresponds with 70% narrowing by the NASCET method. We might expect this estimate of narrowing by BBCMR to be higher than that by the ECST method since the extrapolation in the ECST method would not account for vascular remodeling of the outer wall. Although we suspect BBCMR images are highly reliable for measuring stenosis, this remains to be tested against the reliability of CMRA, and with these additional studies a correction factor might be determined that can relate stenosis measurements based on BBCMR with that of CMRA, the currently accepted clinical standard.

Measures of plaque size may also offer insight into monitoring medical intervention not attainable by angiography. Brown et al. (28) showed that lipid lowering therapy can result in a 75% reduction in adverse coronary events despite a small angiographic change seen in only 12% of lesions. Corti et al. (29) showed that the response to medical therapy can be detected by CMR as a change in plaque size despite no change in luminal narrowing, supporting the use of CMR for accounting for vascular remodeling.

Our study also suggests that BBCMR can be used to detect angiographically occult carotid atherosclerosis, which may occur at a stage in which dietary and lifestyle modifications may be effective in preventing adverse cerebrovascular events (30). A substantial plaque burden may exist even before the lumen is narrowed, but the exact degree of narrowing at which encroachment begins is still unclear (20). We estimate that as much as 67% stenosis by BBCMR may exist before angiography can detect atherosclerosis by diameter-based stenosis measurements. This estimate was only slightly lower (63%) when area-based measurements were used on the CMRA images. Although area- and diameter-based measurements will differ for the same degree of narrowing, the earliest sign of narrowing (i.e., crossing the y-axes in Figs. 3 and 4), whether measured by diameter or

area, should correspond to approximately the same area-based narrowing on corresponding BBCMR images (i.e., 67.3% [95% CI: 60.1, 74.4] versus 63.1% [95% CI: 54.6, 71.6]). This estimate of 67% stenosis should be interpreted with caution since it is extrapolated from more stenotic vessels, and plaques causing low-grade stenosis may behave differently. Kiechl et al. (17) showed that luminal expansion accommodates carotid plaque formation early in its development, but plaque size progressed more rapidly with little or no compensatory enlargement for stenoses above 40%.

The implications of our study might also apply to other vessels prone to plaque formation such as coronary arteries. Retrospective studies of newly occluded coronary arteries that led to acute myocardial infarctions have revealed that most of these lesions were not significantly narrowed prior to the event, with many causing less than 50% stenosis (31–33). Perhaps a greater plaque burden would be uncovered if BBCMR were applied to these vessels.

We postulated that the distal CCA should be used for the reference diameter when determining stenoses for carotid bulb lesions. The 3 carotid bulb lesions had the largest distances between the points of stenosis and the reference diameters, and the stenosis measurements by CMRA for these lesions more closely matched those determined by BBCMR when the CCA was used as the reference diameter (Fig. 5). We cannot draw definitive conclusions based on 3 bulb lesions; nonetheless, our results call for studies with more bulb lesions to confirm that the CCA reference diameter is more suitable than the distal ICA for lesions in this location.

It is noteworthy that BBCMR is not restricted to assessing luminal narrowing at a single point as is done with angiography, but rather it can account for the length of the plaque and determine its volume, limited only by the time it takes to acquire enough slices to include the plaque. Recent studies demonstrated that the plaque volume is relevant to its risk for rupture (34). BBCMR is also capable of characterizing the morphologic components of the plaque (35, 36), its mechanical properties, and the degree of active inflammation that may predict its risk for rupture. These considerations highlight the unique value of BBCMR against ultrasound, which is also capable measuring plaque size unless hampered by shadowing from calcification, but cannot discriminate these features that predict plaque rupture. Juxtaluminal thrombus, an important indicator of plaque rupture or erosion with subsequent cerebrovascular embolic events (37), can be reliably identified using BBCMR (38). Together these factors demonstrate the valuable insight of BBCMR into stroke risk from plaque that goes well beyond that achievable by assessing its hemodynamic effect on the lumen. Prospective studies of these plaque features and the degree of narrowing determined by BBCMR are needed to better understand the clinical implications of these measurements.

CONCLUSION

Measurements of carotid stenosis based on BBCMR appear to avoid the underestimation encountered by lumen assessment techniques, specifically CMRA, since it identifies the outer wall and accounts for the outward remodeling of the vessel during plaque progression that preserves the lumen. Stenosis determined by BBCMR correlates with that measured by CMRA, with 70% stenosis by CMRA, the threshold for surgical management of symptomatic carotid atherosclerosis, corresponding with 89.4% stenosis (95% CI: 85.1, 93.6) by BBCMR area measurements. Furthermore, BBCMR is not subject to the technical limitations of CMRA that tend to overestimate narrowing and can directly visualize the outer wall averting the poor reader reliability of the ECST method. BBCMR could serve as a new measure of carotid narrowing to guide management, but prospective studies are needed to better understand the clinical implications of this new scale of disease.

REFERENCES

1. Beneficial effect of carotid endarterectomy in symptomatic patients with high-grade carotid stenosis. North American Symptomatic Carotid Endarterectomy Trial Collaborators. N Engl J Med 1991;325:445–53.
2. Barnett HJ, Taylor DW, Eliasziw M, Fox AJ, Ferguson GG, Haynes RB, et al. Benefit of carotid endarterectomy in patients with symptomatic moderate or severe stenosis. North American Symptomatic Carotid Endarterectomy Trial Collaborators. N Engl J Med 1998;339:1415–25.
3. MRC European Carotid Surgery Trial: interim results for symptomatic patients with severe (70–99%) or with mild (0–29%) carotid stenosis. European Carotid Surgery Trialists' Collaborative Group. Lancet 1991;337:1235–43.
4. Biller J, Feinberg WM, Castaldo JE, Whittemore AD, Harbaugh RE, Dempsey RJ, et al. Guidelines for carotid endarterectomy: a statement for healthcare professionals from a Special Writing Group of the Stroke Council, American Heart Association. Circulation 1998;97:501–9.
5. Griffiths GD, Razzaq R, Farrell A, Ashleigh R, Charlesworth D. Variability in measurement of internal carotid artery stenosis by arch angiography and duplex ultrasonography–time for a reappraisal? Eur J Vasc Endovasc Surg 2001;21:130–6.
6. Alexandrov AV, Bladin CF, Maggisano R, Norris JW. Measuring carotid stenosis. Time for a reappraisal. Stroke 1993;24: 1292–96.
7. Williams MA, Nicolaides AN. Predicting the normal dimensions of the internal and external carotid arteries from the diameter of the common carotid. Eur J Vasc Surg 1987;1:91–6.
8. Scarabino T, Carriero A, Giannatempo GM, Marano R, De Matthaeis P, Bonomo L, et al. Contrast-enhanced MR angiography (CE MRA) in the study of the carotid stenosis: comparison with digital subtraction angiography (DSA). J Neuroradiol 1999;26:87–91.
9. Remonda L, Senn P, Barth A, Arnold M, Lovblad KO, Schroth G. Contrast-enhanced 3D MR angiography of the carotid artery: comparison with conventional digital subtraction angiography. AJNR Am J Neuroradiol 2002;23:213–9.
10. U-King-Im JM, Trivedi RA, Cross JJ, Higgins NJ, Hollingworth W, Graves M, et al. Measuring carotid stenosis on contrast-enhanced magnetic resonance angiography: diagnostic performance and reproducibility of 3 different methods. Stroke 2004;35:2083–88.
11. Zarins CK, Zatina MA, Giddens DP, Ku DN, Glagov S. Shear stress regulation of artery lumen diameter in experimental atherogenesis. J Vasc Surg 1987;5:413–20.
12. Giddens DP, Zarins CK, Glagov S. The role of fluid mechanics in the localization and detection of atherosclerosis. J Biomech Eng 1993;115:588–4.

13. Tuttle JL, Nachreiner RD, Bhuller AS, Condict KW, Connors BA, Herring BP, et al. Shear level influences resistance artery remodeling: wall dimensions, cell density, and eNOS expression. Am J Physiol Heart Circ Physiol 2001;281:H1380–9.
14. Glagov S, Weisenberg E, Zarins CK, Stankunavicius R, Kolettis GJ. Compensatory enlargement of human atherosclerotic coronary arteries. N Engl J Med 1987;316:1371–5.
15. Steinke W, Els T, Hennerici M. Compensatory carotid artery dilatation in early atherosclerosis. Circulation 1994;89:2578–1.
16. Benes V, Netuka D, Mandys V, Vrabec M, Mohapl M, Benes V Jr, et al. Comparison between degree of carotid stenosis observed at angiography and in histological examination. Acta Neurochir (Wien) 2004;146:671–7.
17. Kiechl S, Willeit J. The natural course of atherosclerosis. Part I: incidence and progression. Arterioscler Thromb Vasc Biol 1999;19:1484–90.
18. Siegel RJ, Swan K, Edwalds G, Fishbein MC. Limitations of postmortem assessment of human coronary artery size and luminal narrowing: differential effects of tissue fixation and processing on vessels with different degrees of atherosclerosis. J Am Coll Cardiol 1985;5:342–6.
19. Yuan C, Beach KW, Smith LH, Jr., Hatsukami TS. Measurement of atherosclerotic carotid plaque size in vivo using high resolution magnetic resonance imaging. Circulation 1998;98:2666–71.
20. Wasserman BA, Wityk RJ, Trout HH, 3rd, Virmani R. Low-grade carotid stenosis: looking beyond the lumen with MRI. Stroke 2005;36:2504–13. Epub 2005 Oct 2520.
21. Edelman RR, Chien D, Kim D. Fast selective black blood MR imaging. Radiology 1991;181:655–60.
22. Wasserman BA, Smith WI, Trout HH, 3rd, Cannon RO, 3rd, Balaban RS, Arai AE. Carotid artery atherosclerosis: in vivo morphologic characterization with gadolinium-enhanced double-oblique MR imaging initial results. Radiology 2002;223:566–73.
23. North American Symptomatic Carotid Endarterectomy Trial. Methods, patient characteristics, and progress. Stroke 1991;22:711–20.
24. Zhang S, Cai J, Luo Y, Han C, Polissar NL, Hatsukami TS, Yuan C. Measurement of carotid wall volume and maximum area with contrast-enhanced 3D MR imaging: initial observations. Radiology 2003;228:200–5.
25. Townsend TC, Saloner D, Pan XM, Rapp JH. Contrast material-enhanced MRA overestimates severity of carotid stenosis, compared with 3D time-of-flight MRA. J Vasc Surg 2003;38:36–40.
26. Cosottini M, Pingitore A, Puglioli M, Michelassi MC, Lupi G, Abbruzzese A, et al. Contrast-enhanced three-dimensional magnetic resonance angiography of atherosclerotic internal carotid stenosis as the noninvasive imaging modality in revascularization decision making. Stroke 2003;34:660–4.
27. Rothwell PM, Gutnikov SA, Warlow CP. Reanalysis of the final results of the European Carotid Surgery Trial. Stroke 2003;34:514–23.
28. Brown BG, Zhao XQ, Sacco DE, Albers JJ. Lipid lowering and plaque regression. New insights into prevention of plaque disruption and clinical events in coronary disease. Circulation 1993;87:1781–91.
29. Corti R, Fuster V, Fayad ZA, et al. Lipid lowering by simvastatin induces regression of human atherosclerotic lesions: two years' follow-up by high-resolution noninvasive magnetic resonance imaging. Circulation 2002;106:2884–7.
30. Markus RA, Mack WJ, Azen SP, Hodis HN. Influence of lifestyle modification on atherosclerotic progression determined by ultrasonographic change in the common carotid intima-media thickness. Am J Clin Nutr 1997;65:1000–4.
31. Little WC, Constantinescu M, Applegate RJ, Kutcher MA, Burrows MT, Kahl FR, et al. Can coronary angiography predict the site of a subsequent myocardial infarction in patients with mild-to-moderate coronary artery disease? Circulation 1988;78:1157–66.
32. Giroud D, Li JM, Urban P, Meier B, Rutishauer W. Relation of the site of acute myocardial infarction to the most severe coronary arterial stenosis at prior angiography. Am J Cardiol 1992;69:729–32.
33. Ambrose JA, Tannenbaum MA, Alexopoulos D, Hjemdahl-Monsen CE, Leavy J, Weiss M, et al. Angiographic progression of coronary artery disease and the development of myocardial infarction. J Am Coll Cardiol 1988;12:56–62.
34. Fujii K, Kobayashi Y, Mintz GS, Takebayashi H, Dangas G, Moussa I, et al. Intravascular ultrasound assessment of ulcerated ruptured plaques: a comparison of culprit and nonculprit lesions of patients with acute coronary syndromes and lesions in patients without acute coronary syndromes. Circulation 2003;108:2473–8. Epub 2003 Nov 2410.
35. Fayad ZA, Fuster V. Clinical imaging of the high-risk or vulnerable atherosclerotic plaque. Circ Res 2001;89:305–6.
36. Yuan C, Zhang SX, Polissar NL, Echelard D, Ortiz G, Davis JW, et al. Identification of fibrous cap rupture with magnetic resonance imaging is highly associated with recent transient ischemic attack or stroke. Circulation 2002;105:181–5.
37. Sitzer M, Muller W, Siebler M, Hort W, Kniemeyer HW, Jancke L, et al. Plaque ulceration and lumen thrombus are the main sources of cerebral microemboli in high-grade internal carotid artery stenosis. Stroke 1995;26:1231–3.
38. Kampschulte A, Ferguson MS, Kerwin WS, Polissar NL, Chu B, Saam T, et al. Differentiation of intraplaque versus juxtaluminal hemorrhage/thrombus in advanced human carotid atherosclerotic lesions by in vivo magnetic resonance imaging. Circulation 2004;110:3239–44.